

## The resonance Raman spectrum of $I_2$ in solution

HERBERT L. STRAUSS

Department of Chemistry, University of California, Berkeley, California 94720, U.S.A.

Received on August 26, 1988.

### Abstract

An extensive set of resonance excitation profiles and the corresponding depolarization dispersion profiles of the vibrational bands of iodine in solution were determined. The results of the experiments are compared to the results of detailed calculations. The calculations are based on the gas phase potentials of iodine. Overall agreement is good for the noninteracting solvents considered here. However, there are a number of discrepancies, which suggest that higher iodine states — perhaps charge transfer states involving the solvent — contribute to the Raman cross section in the visible region of the spectrum. A number of other small effects, such as rotation of iodine in the excited states, also contribute.

**Key words:** Resonance excitation profiles, resonance Raman spectrum, iodine properties.

One day in the Spring of 1969, I knocked at the door of C. V. Raman's residence in Bangalore. I had come despite the warnings of my friends at the I.I.Sc. and the forbidding sign that Raman had erected beside his front gate. However, the Ramans greeted me with enthusiasm and Raman showed me his latest work, while Mrs. Raman made tea. We spent a very enjoyable few hours together. Raman was eager to discuss both his recent work and that of years past. He continued to relish his older work and restate his sometimes controversial positions from long ago. A month later I met with Professor Charles Coulson in Oxford. When I recounted some of Raman's conversation, he said, "That's just what he said to me at a meeting in 1937!" One of Raman's lifelong interests was the color of things, especially his prized flowers. It is with this in mind that I discuss in this paper the effect of changing the color of the excitation on the Raman Effect of the well-known colored solutions of  $I_2$ .

Two observations led to this investigation. The first is the profound changes in the relative intensity of the iodine fundamental and its overtones as the frequency of the exciting laser is changed throughout the visible band. The second and more unusual observation is that the Raman bands apparently shift as the color of the laser is changed (fig. 1)<sup>1</sup>.

The visible spectrum of  $I_2$  is one of the spectra most thoroughly studied by molecular spectroscopy. The electronic states of  $I_2$  have been particularly well characterized in the spectral region that contributes to the visible absorption and fluorescence spectra<sup>2-5</sup>. The potential energy curves for the states that contribute to the visible absorption are

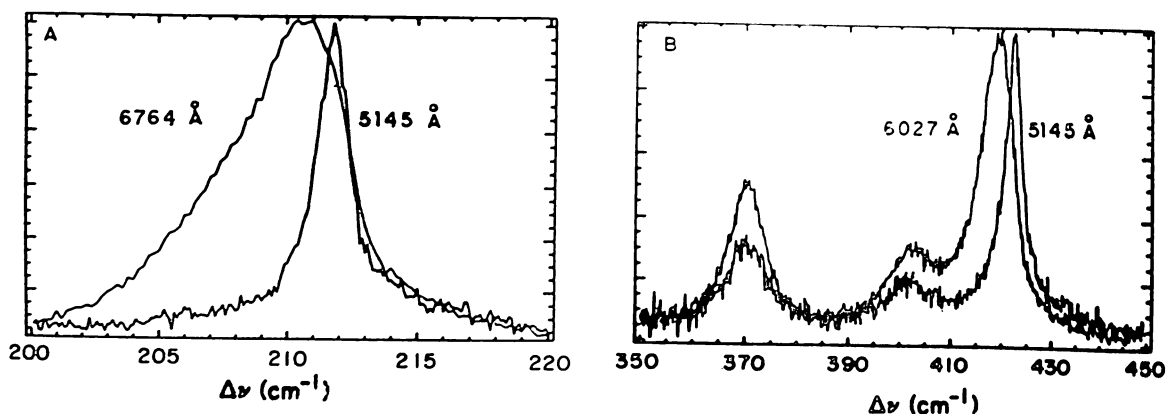


FIG. 1. High-resolution Raman spectra of the fundamental (A) and first overtone (B) of  $I_2$  in *n*-hexane. Each spectrum is labeled with the laser excitation wavelength. The changes that occur in the band shapes and positions are due to the relative resonance enhancements of the hot bands. The frequency scale for each spectrum of the overtone was calibrated relative to the *n*-hexane band at  $370\text{ cm}^{-1}$ . The band at  $402\text{ cm}^{-1}$  is another solvent band.

shown in fig. 2<sup>6</sup>. The low-resolution spectrum of  $I_2$  vapor is shown in fig. 3. The total absorption band is composed of three parts. About 5% of the total absorption is due to the  $A \leftarrow X$  transition, which gives rise to the weak low-frequency wing. At the high-

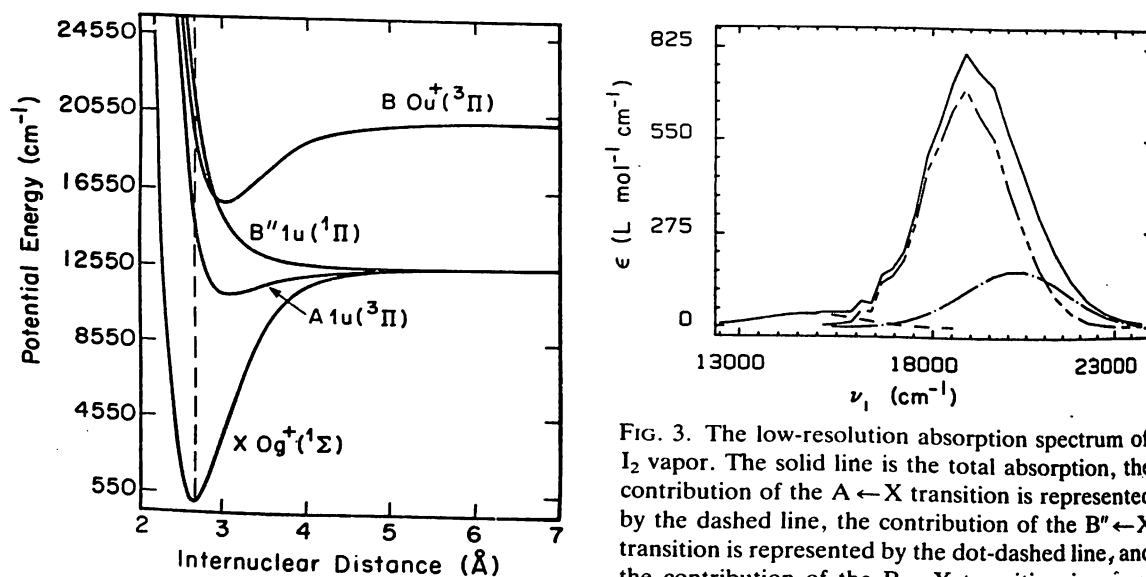


FIG. 2. Potential energy curves for the electronic states of  $I_2$  that contribute to the visible absorption spectrum. The dashed line at  $2.67\text{ Å}$  represents the equilibrium internuclear distance for ground state  $I_2$  (redrawn from ref. 6).

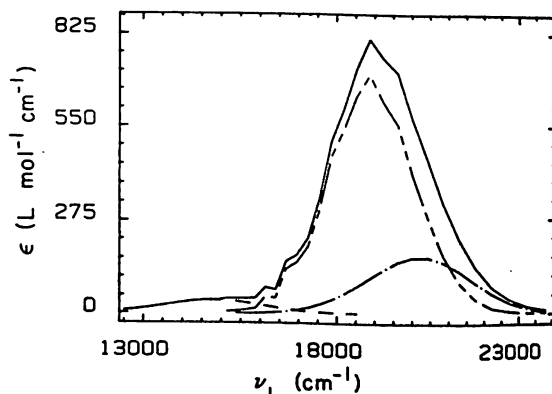


FIG. 3. The low-resolution absorption spectrum of  $I_2$  vapor. The solid line is the total absorption, the contribution of the  $A \leftarrow X$  transition is represented by the dashed line, the contribution of the  $B'' \leftarrow X$  transition is represented by the dot-dashed line, and the contribution of the  $B \leftarrow X$  transition is represented by the dash-dashed line. Note that the difference between the  $A \leftarrow X$  and the total absorption is negligible below  $14,500\text{ cm}^{-1}$ . The total spectrum and the breakdown into contributing transitions are plotted from the table of values in ref. 2. The bumpiness in the  $B \leftarrow X$  spectrum is the result of residual vibrational structure.

frequency side the B'' ← X transition appears, and this accounts for 22% of the absorption. The main B ← X transition accounts for 73% of the absorption.

The properties of iodine in solution have been of interest to scientists for at least a century<sup>7</sup>. Most spectral studies of iodine in solution have dealt with the charge-transfer interactions between I<sub>2</sub> and the solvent<sup>8</sup>. Recently, much attention has been focused on the effect of solvents on the predissociation of I<sub>2</sub> and subsequent recombination of the I atoms<sup>9,10</sup>.

Theory predicts that, in the resonance region, the Raman spectrum of I<sub>2</sub> will depend on the frequency of the laser and on the interaction of the solvent with the excited states of the spectroscopically active molecule. The differential cross section for the Raman cross-section of a randomly oriented gas phase molecule is given by<sup>11-13</sup>

$$\frac{d\sigma}{d\Omega} = \left(\frac{4\pi^2}{hc}\right)^2 \nu_S^3 \nu_L \left| \sum_{\rho\sigma} l_{S\rho} \alpha_{\rho\sigma}(\nu_L, I, F) l_{\sigma L} \right|^2, \quad (1)$$

where the elements of the polarizability tensor,  $\alpha_{\rho\sigma}$ , are given by

$$\alpha_{\sigma\rho}(\nu_L, I, F) = \sum_E \frac{\langle F | \mu \cdot \epsilon_\rho^* | E \rangle \langle E | \mu \cdot \epsilon_\sigma | I \rangle}{\nu_E - \nu_I - \nu_L - i\Gamma_E}. \quad (2)$$

Here  $I$  and  $F$  are the initial and final states of the molecule and the summation over  $E$  is over all the states of the molecule.  $\nu_S$ ,  $\nu_L$ ,  $\nu_E$  and  $\nu_I$  are the energies (in cm<sup>-1</sup>) of the scattered light, the incident laser, the intermediate state  $E$  and the initial state  $I$ , respectively.  $\Gamma$  is the width of the intermediate state. The polarization vectors of the scattered photons,  $\epsilon_\rho$  and the incident photon,  $\epsilon_\sigma$ , are referred to the molecular-fixed frame. The direction cosines  $l_{S\rho}$  and  $l_{\sigma L}$  convert this frame to the laboratory frame of reference. A number of steps are required to convert this formula to usable form. The averages over the direction cosine elements are taken and lead to expressions involving specific components of the  $\alpha$ -tensor. The dipole matrix elements such as  $\langle F | \mu | I \rangle$  are separated into electronic and vibrational parts by invoking the Born-Oppenheimer approximation. Finally, the appropriate index of refraction corrections for the presence of the solvent are made.

The results of the calculations are formulas for the total differential cross-section and for the polarization ratio in terms of the components of the polarizability. For I<sub>2</sub> there are two such components,  $\alpha_{\gamma\gamma}$  where  $\gamma$  is the molecular axis, and  $\alpha_{\beta\beta}$  where  $\beta$  is an axis perpendicular to  $\gamma$ . For the B ← X transition the only non-zero terms are in  $\alpha_{\gamma\gamma}$ , and for the A ← X and B'' ← X transitions only the  $\alpha_{\beta\beta}$  survive. As a consequence, the depolarization ratio would be 1/8 if only the A and B'' states contribute to the Raman cross-section and 1/3 if only the B state contributes.

We have made four types of measurements and compared the results to detailed calculations<sup>13-16</sup>. In doing this, we had two goals in mind. The first is to provide a comprehensive test of the theory of the resonance effect and to resolve various contradictions in

the literature. The second is to determine the properties of the excited states of  $I_2$  in solution. As we shall see, the information available from resonance Raman spectroscopy is complementary to that from absorption spectroscopy.

The four types of measurements are: (1) The resonance excitation profile, REP; that is, the change of intensity of the various  $I_2$  Raman bands as a function of the frequency of the exciting laser. This measurement was done in *n*-hexane, a rather non-interacting solvent. (2) The depolarization dispersion profiles which we call DDPs; that is, the variation of the depolarization ratio *versus* frequency of the exciting laser. (3) The REPs in other non-interacting solvents. (4) The variation of the band shapes of the  $I_2$  Raman spectrum with laser frequency.

It is worthwhile to digress to consider the theory of the resonance Raman Effect further. In eqn (2), the  $\Gamma$  in the denominator is the lifetime of the excited state for a gas phase molecule. For a molecule in condensed phase, the correctness of using  $\Gamma$  to account for interactions with the surroundings is not so clear. We followed the formulation of Mukamel<sup>17</sup> which shows that  $\Gamma$  is  $1/T_2$  for the intermediate state. Mukamel's

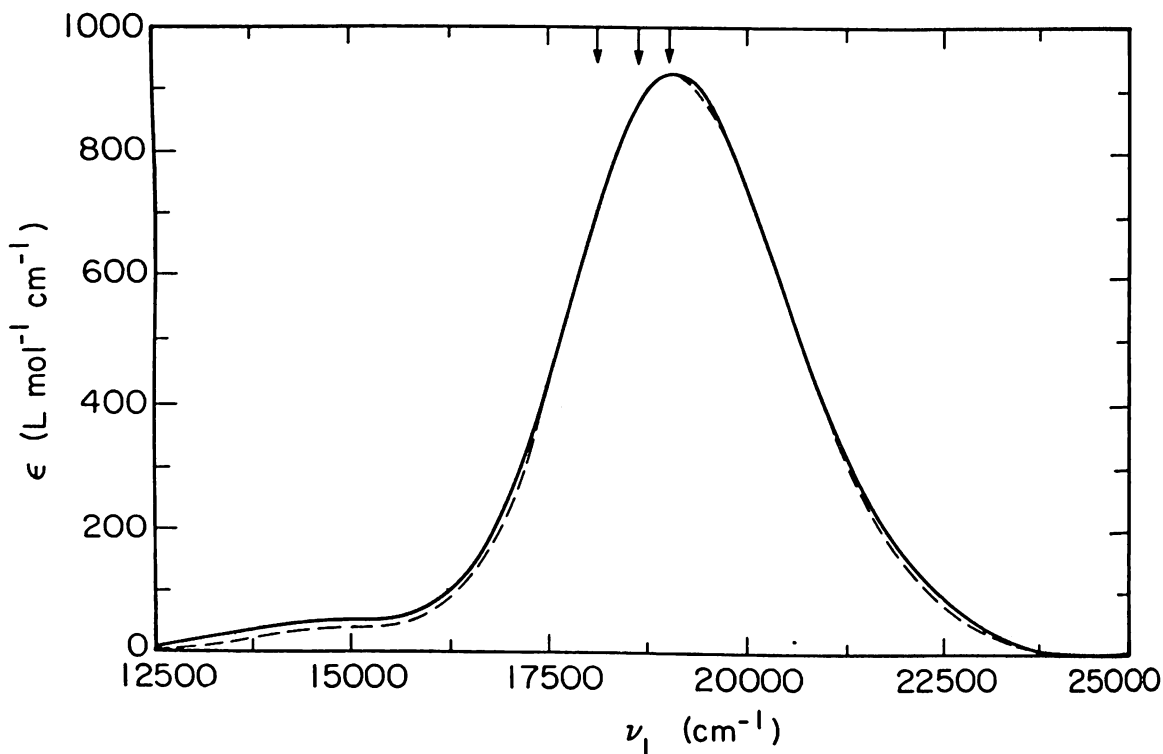


FIG. 4. The experimental (dashed line) and calculated (solid line) visible absorption spectrum of  $I_2$  in *n*-hexane. The anharmonic ground state, discussed in the text, was used for all calculations of  $I_2$  in *n*-hexane. The calculation parameters are:  $\Gamma = 20 \text{ cm}^{-1}$ ;  $\theta$ , the inhomogeneous width,  $= 400 \text{ cm}^{-1}$ ; and  $T = 300 \text{ K}$ . The calculated spectrum is fairly insensitive to  $\Gamma < 100 \text{ cm}^{-1}$ . The intensity of the B state absorption was matched using  $L^2 = 1.75$  as a solution correction factor. The width of the spectrum was matched by adjusting  $\theta$ . The calculated spectrum fits less accurately in the high and low frequency wings where the A and B'' states dominate.

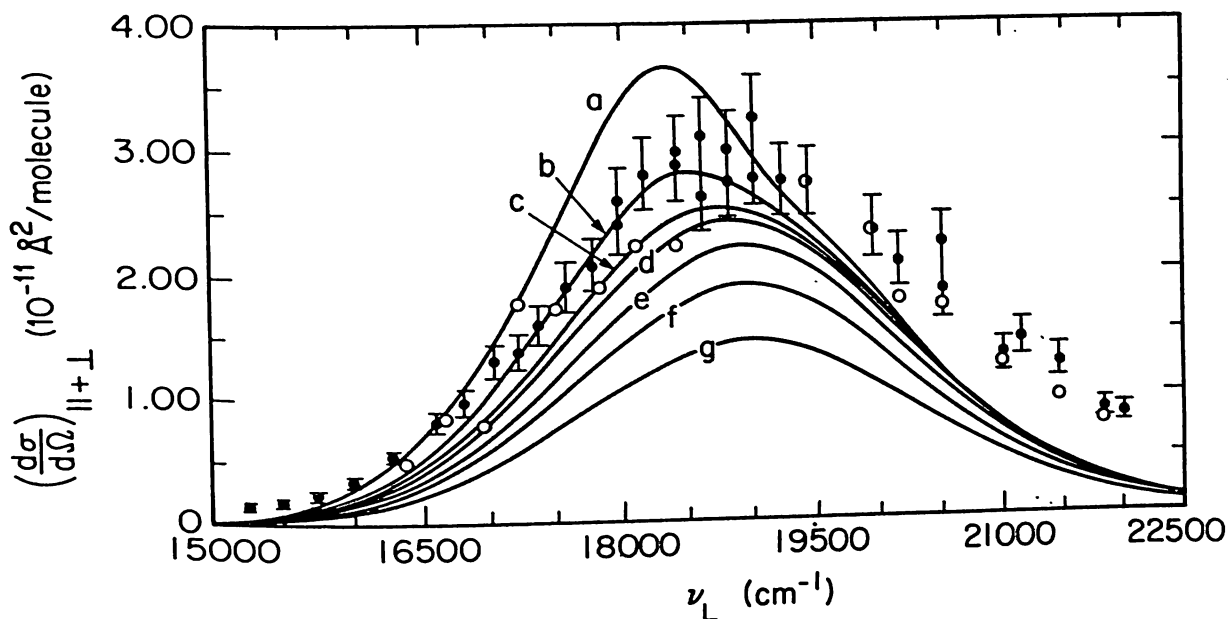


FIG. 5. Calculated and experimental REPs for the I<sub>2</sub> fundamental in *n*-hexane plotted on an absolute scale. The data points with error bars are our experimental values (the error bars shown are  $\pm 10\%$ ). The results of repeated experiments are shown as multiple data points. The open circles represent data points from Rousseau *et al.*<sup>19</sup>. These points were scaled to our value of the absolute cross section at 5145 Å. The homogeneous linewidths, or damping factors, are as follows:  $\Gamma =$  (a) 10 cm<sup>-1</sup>, (b) 15 cm<sup>-1</sup>, (c) 20 cm<sup>-1</sup>, (d) 25 cm<sup>-1</sup>, (e) 50 cm<sup>-1</sup>, (f) 100 cm<sup>-1</sup>, and (g) 200 cm<sup>-1</sup>. The inhomogeneous linewidth and the solvent effect on the transition strength are both determined by the absorption spectrum.

formulas contain separate terms for the resonance Raman scattering and the resonance fluorescence. The latter is very broad and we ignore it in what follows.

The total resonance Raman intensity varies with  $\Gamma$  in stark contrast to total intensity of an absorption spectrum, which is of course invariant to the width of the states. Thus a measurement of the absolute intensity of the Raman Effect determines  $\Gamma$ , provided we have a model of the vibronic states that allows us to calculate the matrix elements of eqn (2). To determine these, we assume that the electronic states of I<sub>2</sub> are the same in hexane as they are in the gas phase. However, we do modify the ground state vibrational states in hexane and the other solvents we have used to match the observed anharmonicity for each one<sup>18</sup>. Our calculations match the observed absorption spectrum well, as shown in fig. 4<sup>19</sup>.

We take up the Raman Effect experimental results in order. Figure 5 shows the resonance excitation profile for the I<sub>2</sub> fundamental. Also on the figure are the results of calculations which we discuss in a moment. Figure 6 shows the data for the first and second overtones of I<sub>2</sub>. In applying the gas phase electronic data to the solution spectra, we chose a value of  $\Gamma$  to give the best fit. The best choice for  $\Gamma$  is about 20 cm<sup>-1</sup> and gives an excellent overall fit, but there are a number of discrepancies. Note that the experimental points are higher than calculated ones at the high-frequency side of the REP of the fundamental and at the peak of the REP of the first overtone.

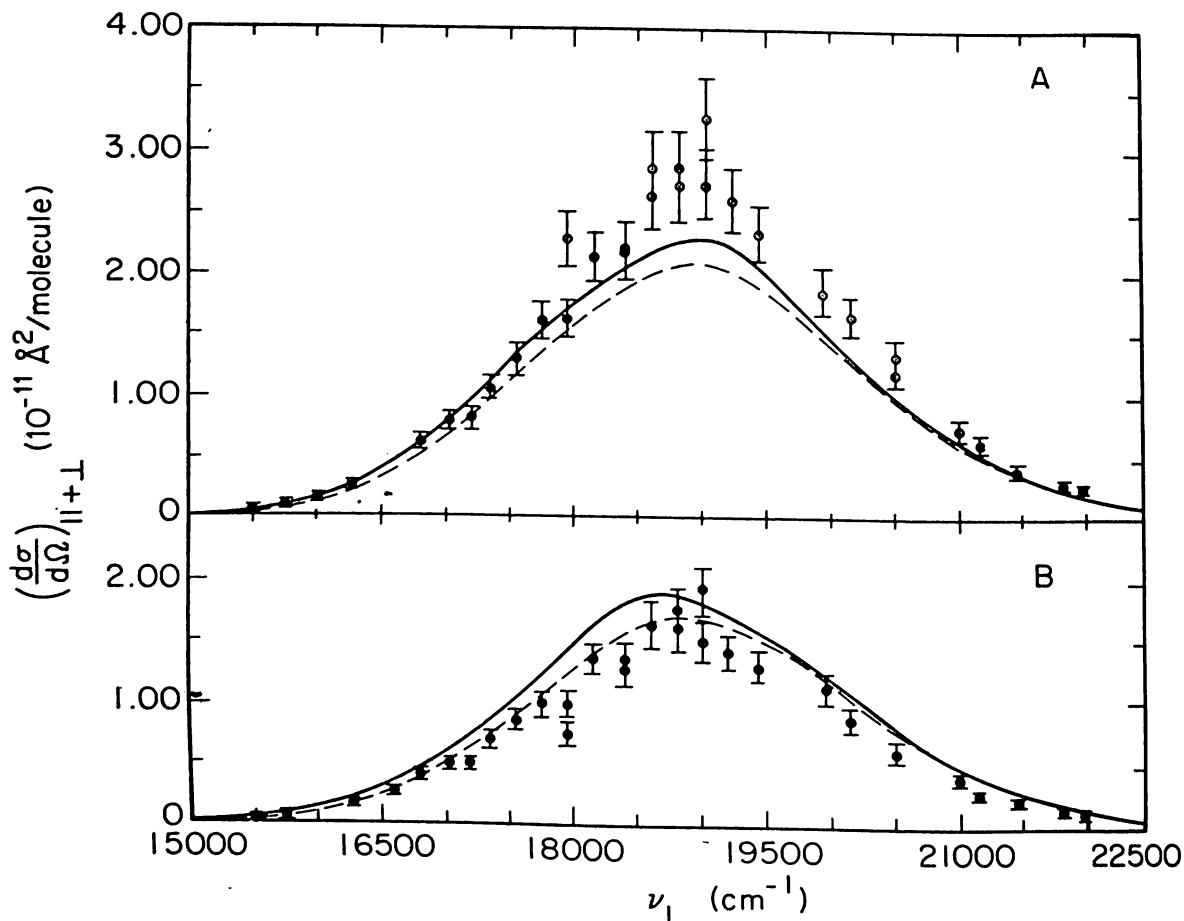


FIG. 6. Calculated and experimental REPs for the  $I_2$  first (A) and second (B) overtones in  $n$ -hexane. The error bars on the experimental points are  $\pm 10\%$  as in fig. 5. The parameters for the calculations are  $\Gamma = 20\text{ cm}^{-1}$  (dashed lines) and  $\Gamma = 15\text{ cm}^{-1}$  (solid lines). Note that  $\Gamma$  is the only adjustable parameter and the ordinate scale is absolute.

To obtain a better fit, we consider the depolarization dispersion profiles and also vary the calculations systematically to test various effects of the solution excited states. Figure 7 shows the new calculations with the same data for the REP of the fundamental. Also shown is the DDP of the fundamental. Near the center of the absorption bands the DDP is almost  $1/3$ , the value for the B state alone, as expected. At the low- and high-frequency wings of the band the DDP changes away from  $1/3$  as the A, B', and other degenerate states participate. We show similar information for the first overtone in fig. 8. In an attempt to resolve the discrepancies mentioned, we included the contribution from the D state in the calculation. The D state is at much higher energy in the isolated  $I_2$  molecule — at about  $54,000\text{ cm}^{-1}$ . It contributes to the Raman spectrum near the  $I_2$  visible absorption band through the B-D cross term that appears in the expression for the polarizability squared. As seen in figs 7 and 8, the fundamental REP is still in disagreement as before, but the overtone REP is in rather better agreement. This is partly due to a recalibration of the absolute intensity, which is based on comparison with

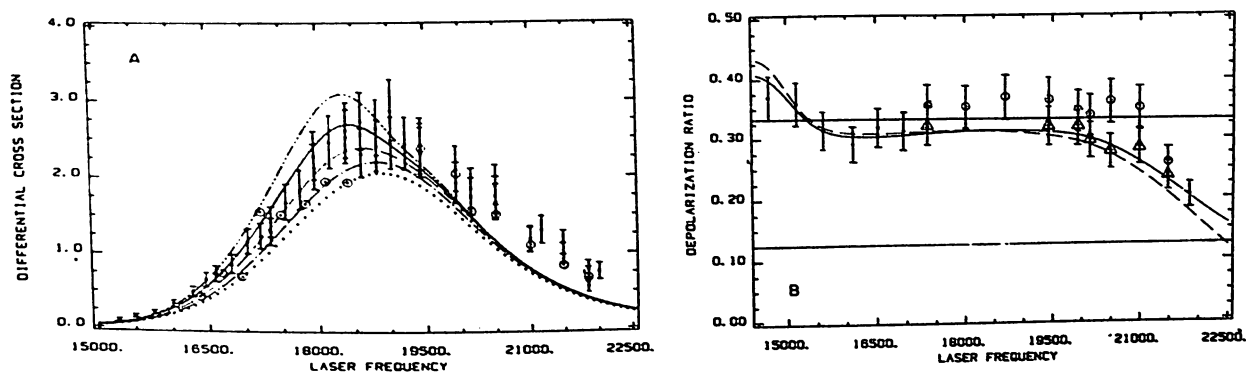


FIG. 7. (A) Calculated and experimental REPs for the  $I_2$  fundamental in hexane plotted on an absolute scale, as in fig. 5 but with more data points and 15% error bars. These points were rescaled to our value of the absolute cross section at 5145 Å. The homogeneous linewidths, or damping factors, are as follows: ——— 12  $cm^{-1}$ , — 15  $cm^{-1}$ , - - 20  $cm^{-1}$ , — · — 30  $cm^{-1}$ , and + + + 50  $cm^{-1}$ . The inhomogeneous linewidth and the solvent effect on the transition strength are both determined by the absorption spectrum. The D state is included in the calculation. (B) The calculated and experimental depolarization dispersion curves of the  $I_2$  fundamental in hexane. The circled data points between 17,000 and 21,500  $cm^{-1}$  represent the raw data at these frequencies. The triangles represent normalized data. Below 17,000  $cm^{-1}$  and above 21,500  $cm^{-1}$  there was no need to normalize the data. The error bars are drawn to  $\pm 10\%$ . The calculation parameters are as in (A) with  $\Gamma = 15 cm^{-1}$ . The solid line includes the D state contribution, while the dashed line neglects this contribution. The horizontal lines at 1/3 and 1/8 represent the depolarization ratios if only nondegenerate or doubly degenerate states, respectively, contribute to the Raman cross-sections.

the benzene 992 band. The calculated DDPs are in better agreement for the fundamental than for the first overtone (fig. 8) or the second overtone (not shown).

Various possibilities were tried to resolve the discrepancies between theory and calculation. Perhaps the most interesting of these considers the addition of an iodine-solvent charge-transfer state to the set of Raman-active states in order to raise the REP in the high-frequency wing. This possibility is subject to experimental test. We repeated our REP measurements in perfluorohexane and in chloroform<sup>15</sup>. Hexane is thought to have a contact charge-transfer state with  $I_2$  in contrast to perfluorohexane, which is not

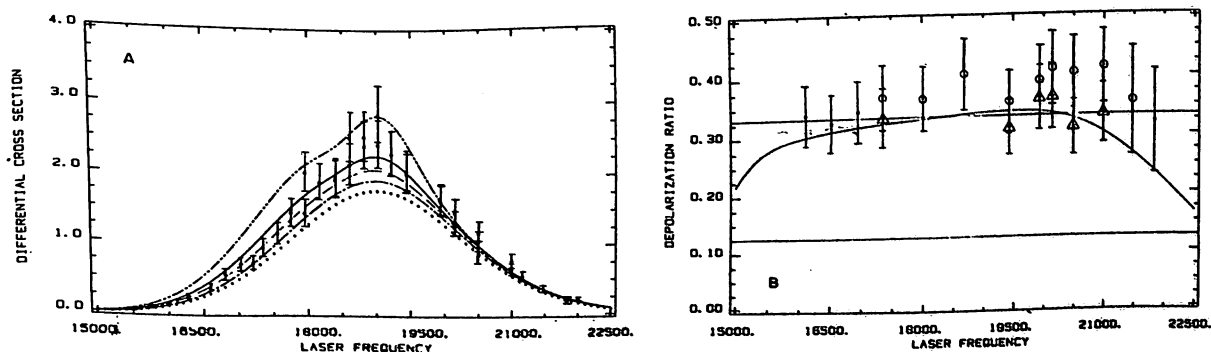


FIG. 8. The calculated and experimental REPs for the first overtone of  $I_2$  in hexane. The error bars are drawn to  $\pm 15\%$ . The parameters are the same as in fig. 7 except that the ——— curve was calculated with  $\Gamma = 10 cm^{-1}$ .

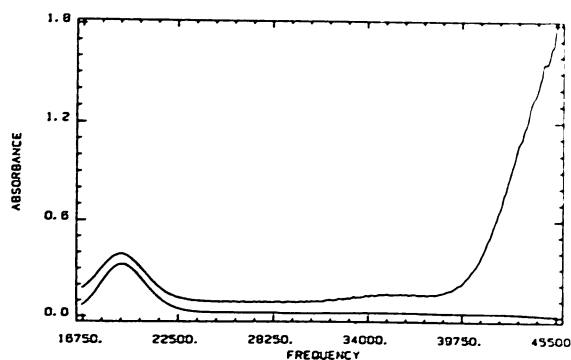


FIG. 9. The UV-visible absorption spectrum of  $I_2$  in *n*-hexane and in perfluorohexane. The top spectrum is  $I_2$  in *n*-hexane which has been offset by 0.08 absorbance units to distinguish the two spectra. Note the strong absorption band appearing in the UV spectrum of  $I_2$  in hexane but not in the spectrum of  $I_2$  in perfluorohexane.

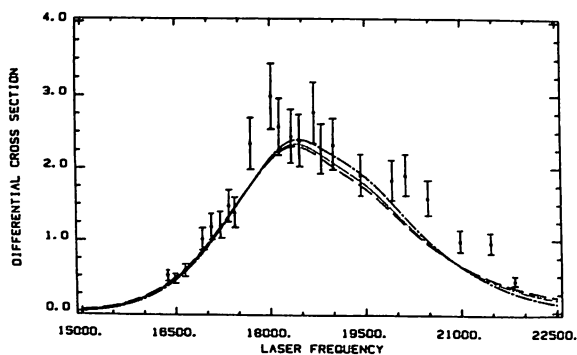


FIG. 10. The calculated and experimental REPs of the  $I_2$  fundamental in perfluorohexane. The error bars are drawn to  $\pm 10\%$ . The curves were all calculated with  $\Gamma = 15 \text{ cm}^{-1}$ . The dashed line was calculated with the D state contribution with  $|\mu_{XD}|^2 = 40 D^2$ , the solid line was calculated with  $|\mu_{XD}|^2 = 25 D^2$ , and the dot-dashed line was calculated with no D state contribution.

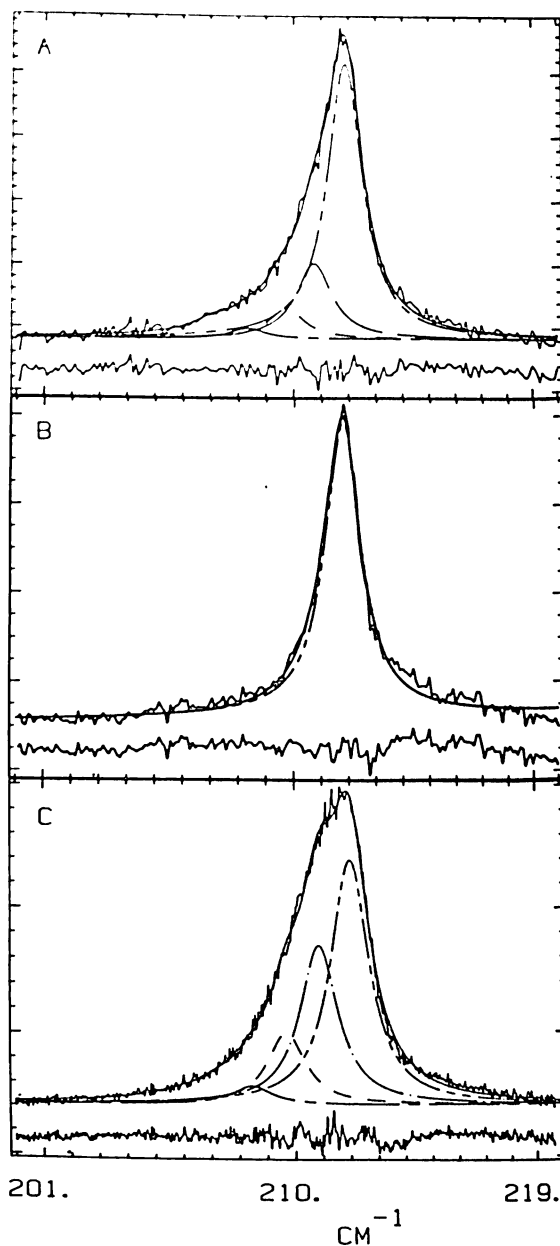


FIG. 11. Raman spectra of the  $I_2$  fundamental fit with Lorentzian lines spaced according to the known anharmonicity of  $I_2$  in hexane. The difference between the experimental spectrum and the total fit is plotted to scale beneath each spectrum. The contributions from the various initial states are as follows:  $i = 0$  (-----),  $i = 1$  (-·-·-·-),  $i = 3$  (----) and  $i = 4$  (-----). The excitation frequencies are (A)  $4579 \text{ \AA}$  ( $21,840 \text{ cm}^{-1}$ ), (B)  $5145 \text{ \AA}$  ( $19,435 \text{ cm}^{-1}$ ), and (C)  $5945 \text{ \AA}$  ( $16,810 \text{ cm}^{-1}$ ).



thought to have one<sup>20</sup>. Chloroform should, of course, have a stronger charge-transfer complex than hexane. Figure 9 shows the UV-visible absorption spectrum of I<sub>2</sub> in both *n*-hexane and in perfluorohexane. It shows the absorption from the charge-transfer complex in hexane and the lack of such an absorption in perfluorohexane.

Figure 10 shows the REP of I<sub>2</sub> in perfluorohexane together with the results of the appropriate calculations. Calculations were again tried both with and without including the possible contribution of the D state. As the figure shows, the experimental points are higher than the theoretical ones, just as for the data in hexane. The results for chloroform are very similar.

It is remarkable that the fit of theory and experiment are so similar for the REPs of I<sub>2</sub> in *n*-hexane, *n*-perfluorohexane and chloroform. All of these give a width of about 15 cm<sup>-1</sup> for the levels of the upper electronic states. This suggests that the width is due to simple thermal fluctuations of the solvents since the three solvents do not differ much in the magnitude of these fluctuations.

Let us go back and consider the curious phenomenon we mentioned at the beginning: the I<sub>2</sub> Raman bands shift with a change in exciting frequency. In all the work mentioned so far, we took spectra at relatively low resolution and ignored any small shifts. Now we consider spectra taken at higher resolution (fig. 1). Each Raman band is made up of both a transition to the ground vibrational state (for example, 1 ← 0) but also hot bands (2 ← 1, 3 ← 2, 2 → 3, etc.). Figure 11 shows a fit of such a hot band sequence to the observed bands taken with different exciting frequencies. It shows that the components that make up an individual vibration shift drastically with excitation and so appear to shift the vibrational band.

The observed bands can be resolved into components at each exciting frequency and so we can derive REPs for each component. Again we can compare with the results of calculations; such a comparison for the fundamental over a part of the frequency range is shown in fig. 12. Discrepancies between experiment and calculation are obvious at the low-frequency side of the data. Agreement is good in the middle and high-frequency side (not shown) and for the first overtone (not shown).

It is difficult to appreciate the details of the small shifts in the calculated REPs and DDPs due to a variety of causes and to compare all of these to the experimental results. Much more detail is available in the original papers<sup>13-16</sup>. Here, we summarize the highlights of our studies.

We have measured the REPs of the fundamental and first two overtones of I<sub>2</sub> in *n*-hexane and placed these profiles on an absolute intensity scale. We have also measured the absolute REP of the I<sub>2</sub> fundamental in perfluorohexane and placed the previously reported REPs of chloroform on an absolute intensity scale. We have measured both the depolarization dispersion profiles and relative intensities of the hot bands in the I<sub>2</sub> bands in hexane. We have compared all of these to calculations, based on gas phase values of the excited state parameters.

In all three solvents, the REPs fit best with an excited state homogeneous width of about 15 cm<sup>-1</sup>, which translates into 0.3 ps. For each fundamental REP, the major

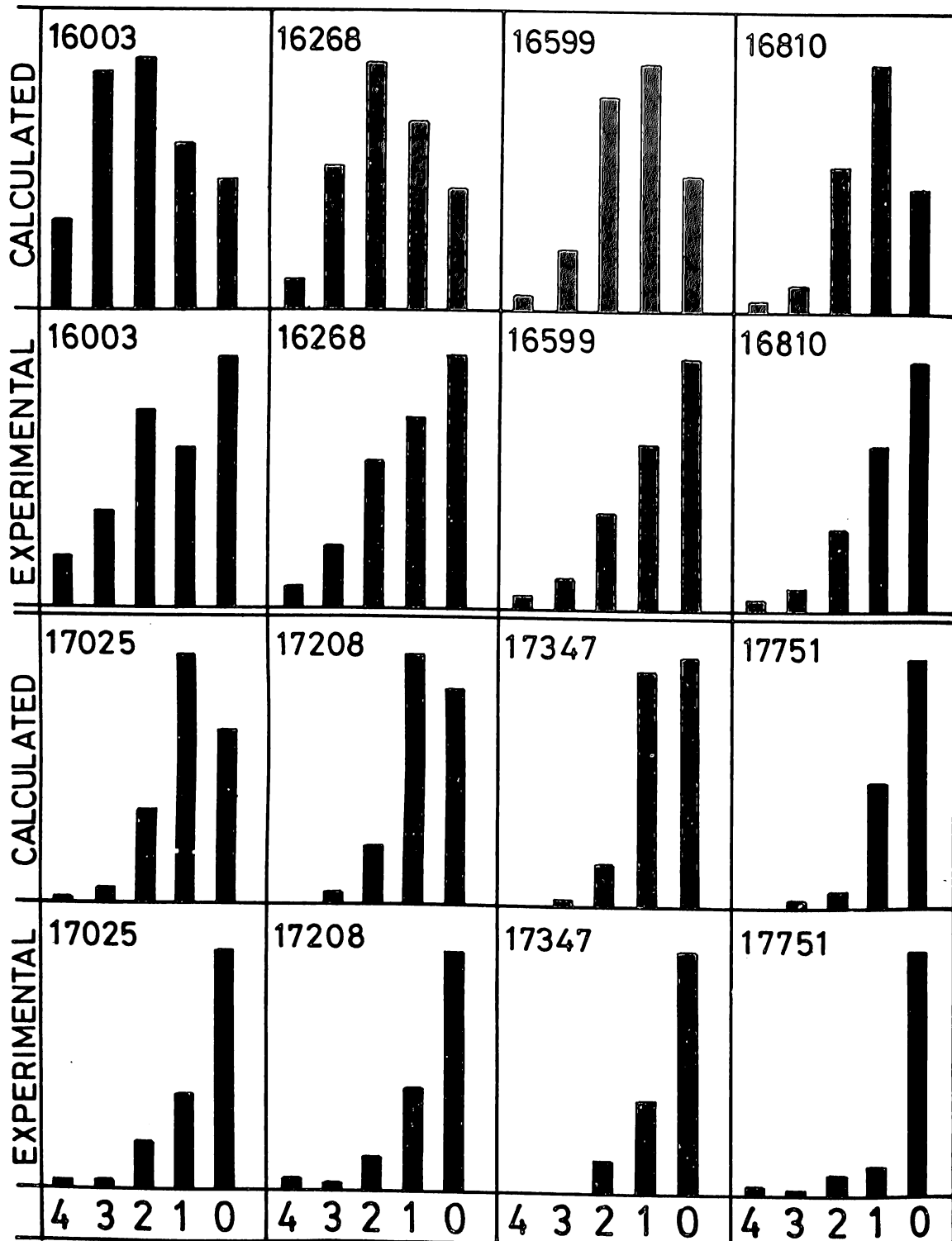


FIG. 12. The calculated and experimental bandshapes for the isotropic part of the  $I_2$  fundamental. The intensity of the strongest transition at each listed excitation frequency is assigned a value of one, and the other transitions are drawn to this scale. The transitions are numbered by indicating the lower vibrational state.  $\Gamma = 15\text{cm}^{-1}$  and the D state is included in the calculation.

discrepancy between calculation and experiment is in the high-frequency wing of the I<sub>2</sub> visible absorption band.

The calculated and experimental depolarization dispersion profiles are in good agreement, if it is assumed that the B'' state is blue shifted about 100 cm<sup>-1</sup> relative to the B state. We note that this small 'shift' may well be due to inaccuracies in the gas phase values or to a solution shift. The consistently high experimental depolarization ratios are also explained, in part, by rotation of the I<sub>2</sub> molecule in the excited electronic state. The intensity distributions of the ground and hot band transitions show good agreement for the first overtone, but again there is disagreement for the fundamental.

It appears that there is a contribution missing from the calculation for the fundamental. Although the addition of another state to the calculation would tend to increase the intensity in the wings as needed to approve agreement, it would all decrease the peak of the REP. This would result from the effect of the cross term between the new state and the B state. Such a decrease is not observed. However, the addition of contributions from a number of further states plus small shifts in the I<sub>2</sub> potentials from those that occur for the isolated molecule will undoubtedly fit our data. More data are needed. The most useful would be in the UV region where the additional states are expected to lie. Another interesting direction is to consider the REPs and DDPs of much stronger I<sub>2</sub>-benzene complexes, a direction we are now pursuing.

### Acknowledgments

Dr. Roseanne J. Sension and Mr. Takamichi Kobayashi did the many painstaking experiments presented here. Dr. Sension developed and carried out the extensive calculations and put theory and experiment together. The National Science Foundation supported this work.

### References

1. SENSON, R. J., SNYDER, R. G. AND STRAUSS, H. L. *Proc. Ninth Int. Conf. Raman Spectroscopy*, Tokyo, Japan, 1984, pp. 646-647.
2. TELLINGHUISEN, J. *J. Chem. Phys.*, 1982, **76**, 4736-4744; 1973, **58**, 2821.
3. MULLIKEN, R. S. *J. Chem. Phys.*, 1971, **55**, 288-309.
4. COXON, J. A. *Mol. Spectrosc.*, 1973, **1**, 177.
5. LUC, P. *J. Mol. Spectrosc.*, 1980, **80**, 41-55.
6. BERGSMAN, J. P., BERENS, P. H., WILSON, K. R., FREDKIN, D. R. AND HELLER, E. J. *J. Phys. Chem.*, 1984, **88**, 612-619.

7. a. BECKMANN, E. *Z. Phys. Chem.*, 1890, **5**, 76-82.  
b. HILDEBRAND, J. H. *J. Am. Chem. Soc.*, 1909, **31**, 26-31.  
AND GLASCOCK, B. L.  
c. BENESI, H. A. AND *ibid*, 1949, **71**, 2703-2707.  
HILDEBRAND, J. H.
8. MULLIKEN, R. S. AND *Molecular complexes*, Wiley, New York, 1969, especially pp. 156-161.  
PERSON, W. B.
9. HYNES, J. T. *Ann. Rev. Phys. Chem.*, 1985, **36**, 573-597.  
*Phys. Rev. Lett.*, 1985, **54**, 951-954.
10. a. BERG, M.,  
HARRIS, A. L. AND  
HARRIS, C. B.  
b. HARRIS, A. L.,  
BROWN, J. K. AND  
HARRIS, C. B. *Ann. Rev. Phys. Chem.*, 1988, **39**, 341.
11. SAKURAI, J. J. *Advanced quantum mechanics*, Addison-Wesley, Reading, Mass, 1967, Ch. 2.
12. YARIV, A. *Quantum electronics*, Wiley, New York, 1975, Ch. 8.
13. SENSION, R. J. AND *J. Chem. Phys.*, 1986, **85**, 3791-3806.  
STRAUSS, H. L.
14. SENSION, R. J., *J. Chem. Phys.*, 1987, **87**, 6221-6232.  
KOBAYASHI, T. AND  
STRAUSS, H. L.
15. SENSION, R. J., *J. Chem. Phys.*, 1987, **87**, 6233-6239.  
KOBAYASHI, T. AND  
STRAUSS, H. L.
16. SENSION, R. J. AND *J. Chem. Phys.*, 1988, **88**, 2289.  
STRAUSS, H. L.
17. MUKAMEL, S. *J. Chem. Phys.*, 1985, **82**, 5398-5408.
18. KIEFER, W. AND *J. Raman Spectrosc.*, 1973, **1**, 417.  
BERNSTEIN, H. J.
19. ROUSSEAU, D. L., *Topics in current physics*, Springer, Berlin, 1979, Vol. 11, Ch. 6.  
FRIEDMAN, J. M. AND  
WILLIAMS, P. F.
20. EVANS, D. F. *J. Chem. Phys.*, 1955, **23**, 1424-1428.